CERN-ATS-Note-2012-002 TECH

2012-01-11

giovanni.de.michele@cern.ch

Power Coupler Simulations for the Linac4 Drift Tube Linac

G. De Michele, F. Grespan, S. Ramberger / BE-RF

Keywords: Linac4 – DTL – prototype

Summary

The power coupler is a crucial element in the design of an RF cavity. Power from an RF source is transported towards the cavity by a waveguide and transferred into the cavity by means of a power coupler that is adapted to both the transport mode in the waveguide and the principal resonant mode in the cavity. In the case of Linac4, a rectangular half-height waveguide (WG) WR2300 is used and the connection from this WG to the cavity is achieved by iris coupling through an interconnecting waveguide (IWG) in the tank wall. In this note simulations and measurements on a prototype and studies on Tank1 of the Linac4 Drift Tube Linac (DTL) are discussed in order to define the dimensions of this IWG such that it optimises the power transfer into the cavity.

1. Introduction

The choice of the iris coupler for the Linac4 DTL follows the design for the CCDTL [1]. Figure 1 shows the dimensions of the iris coupling used for the CCDTL and PIMS structures for Linac4. First measurements with such an iris were done on the DTL prototype [2] using the coupler with the same short circuit that was optimized for the CCDTL earlier. After the installation of the coupler, the height of the interconnecting waveguide (IWG) was found to be 78 mm (Figure 1). Measurements of the prototype have been undertaken in this setup and compared to 3D electromagnetic (EM) simulations in order to get reliable results for the Linac4 Tank1.

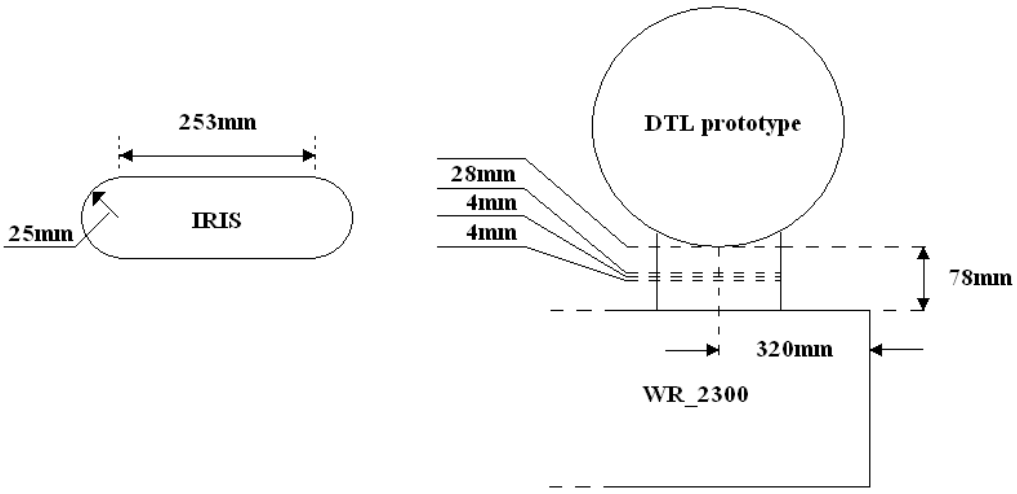

Figure 1 Layout of the cavity connected to the WG through the IWG (right) and iris geometry (left).

2. Measurement set-up

Low power measurements on the Linac4 DTL prototype have been performed in order to determine the resonance frequency, the quality factor Q_{cav} of the cavity and waveguide-to-cavity coupling parameter β of the iris coupler. The Q_{cav} has been determined using two pick-ups that are permanently installed on the prototype for low power measurements and RF monitoring during high power operation. The coupling parameter β has been deduced from measurements of the unloaded and loaded quality factors Q_{cav} and Q_L. The loaded quality factor Q_L is measured with one pick-up on the cavity and one on a waveguide transition (N to WR2300) that is connected to the waveguide. (See [3] for details on low power measurements.)

3D simulations using CST MICROWAVE STUDIO® (CST MWS) and ANSYS HFSS™ (HFSS) confirm the measurements. Only cells 7 and 8 of the prototype are simulated because of their location just above the iris coupler. Simulation results are then scaled to the measured real power dissipation of the full prototype (see section 2.1).With each simulation code, two different methods were applied. For CST MWS, a) the eigenmode solver for lossless structures was used to determine the external Q and the unloaded Q in a post-processing step from surface currents and material properties leading to the coupling parameter β, b) Balleyguier's method was applied running two lossless eigenmode simulations once with perfect magnetic and once with perfect electric boundary conditions at a reference plane set on the waveguide [4].

For HFSS a) a driven modal simulation is used in which the tank, the drift tubes, the stems and the iris coupler are dissipative (copper conductivity $\sigma = 5.8 \times 10^7$ S·m), while the waveguide is supposed to be lossless. The 3D code computes directly the Standing Wave Ratio (SWR) and the scattering parameter S_{11}. The coupling parameter β is extracted from these quantities [3]. As alternative b) again Balleyguier's method is used. The mesh is kept the same in simulations a) and b). The results are combined in order to obtain the external quality factor Q_{ext} of the iris coupler and from this $\beta = Q_{cav}/Q_{ext}$ is calculated. The geometries for HFSS simulations are shown in Figure 2.

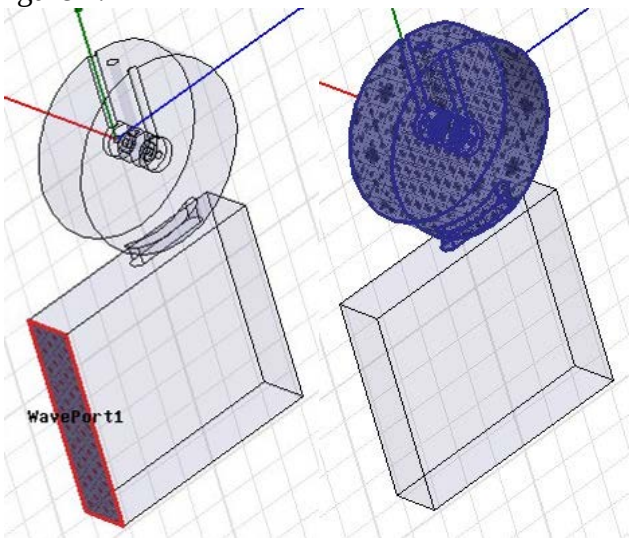

Figure 2 Geometry of the waveguide, the coupler and the cavity with two cells as used in simulations of the coupling parameter β with HFSS. On the left, the reference wave port is highlighted. On the right, dissipative surfaces used in driven modal simulations are shown.

2.1 DTL prototype simulations

As mentioned above, the simulations of the waveguide coupling for the prototype cavity have been performed with a cavity that was reduced to cells 7 and 8. In order to take the whole prototype volume into account for the calculation of the coupling strength, a scaling factor has

been used. The coupling strength is the ratio between the external power and the dissipated power in the cavity; since the external power is always the same (because of the fixed geometry) the coupling strength is given by:

$$\beta_{\text{cav}} = \beta_{7-8,MWS} \cdot \frac{P_{7-8,SF}}{P_{\text{cav},SF}}$$

The power dissipated into the two cells (7-8) can be calculated by Superfish as well as the power dissipated in the whole cavity (Table 1). It is worthwhile noting that in the real structure the dissipated power can be different from the design value because of a difference in the quality factor *Q*. In this case, P_{cav} needs to be corrected by taking the real *Q* value into account. For the DTL prototype the measured *Q* is 80% of the design value (Table 2) and the scaling factor is thus given by:

$$\text{Scaling factor} = 0.8 \frac{P_{7-8,SF}}{P_{\text{cav},SF}}$$

Table 1 Main parameters for the simulated structure.

		***f* [MHz]**	***Q*$_0$**	***P*$_{diss}$ [kW]**	***U* [Joule]**
Cell 7-8	Superfish	351.940	24300	48.7	0.54
	CST MWS	349.328	24408	48.4[1]	1
Prototype	Superfish	351.811	42605	179.0[2]	3.47

Table 2 Scaling factor.

***P*$_{7\text{-}8,sim}$[kW]**	***P*$_{cav,sim}$[kW]**	***P*$_{cav,meas}$/*P*$_{cav,sim}$[%]**	**scaling factor**
48.7	179.0	80	0.218

Simulation results for the coupling strength are listed in Table 3 in comparison with measurements. In the worst case, the agreement between simulations and measurements of the coupling strength is within 10% and between simulations within 6%. The most accurate results were obtained with Balleyguier's Method. The agreement between simulations and measurements on the DTL prototype has been useful to validate the set-up of the simulations for the DTL Tank1.

Table 3 Waveguide-to-cavity coupling parameter.

β	**CST MWS**	**HFSS**	**Measurements**
Code solver	0.93	0.95	0.88
Balleyguier's Method	0.87	0.93	

[1] $P_{diss} \approx P_{CST\ MWS}/2 \cdot U_{SF}/U_{CST\ MWS}$

[2] Taking into account the 80% of the *Q* one obtains 223.7 kW

2.2 DTL Tank1 simulations

After the validation of the simulation method as described above, the same simulations have been performed for DTL Tank1. Here only CST MWS was used to perform the simulations. The simulated volume comprises the 22nd and 23rd cell. The installed waveguide is the half-height WR-2300. The short circuit is 32 cm away from the centre of the coupling hole ($\lambda_{WG}/4$ = 31 cm, see Figure 1). This length was chosen in order to have the reflected wave from the short circuit in phase with the forward wave and to maximize the power going into the cavity.

The results are listed in Table 4. A layout of the structure is shown in Figure 3. Note that for the design, the power transferred to the beam must be taken into account. Assuming the design value of 1 MW of total power, the scaling factor for the calculation of the coupling strength is 0.0432.

Table 4 Main parameters for the simulated structure.

		***f* [MHz]**	***Q*$_0$**	***P*$_{diss}$ [kW]**	***U* [Joule]**
Cell 22-23	Superfish	353.750	28171	43.2	0.55
	CST MWS	350.977	29818	40.7[3]	1
Tank1	Superfish	353.768	50965	528.9[4]	12.18

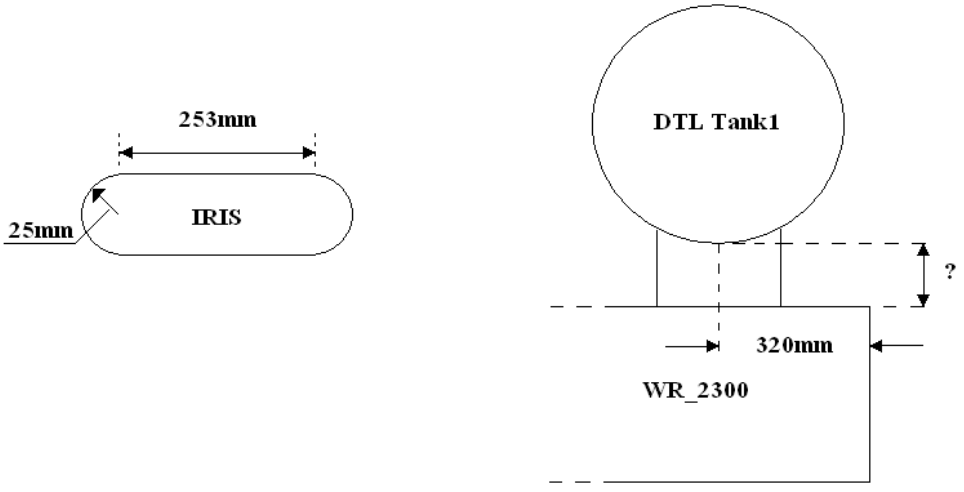

Figure 3 Layout of the cavity connected to the WG through the IWG (right) and iris geometry (left)

[3] $P_{diss} \approx P_{CST\ MWS}/2 \cdot U_{SF}/U_{CST\ MWS}$

[4] Taking into account the 80% of the *Q* one obtains 661.1 kW

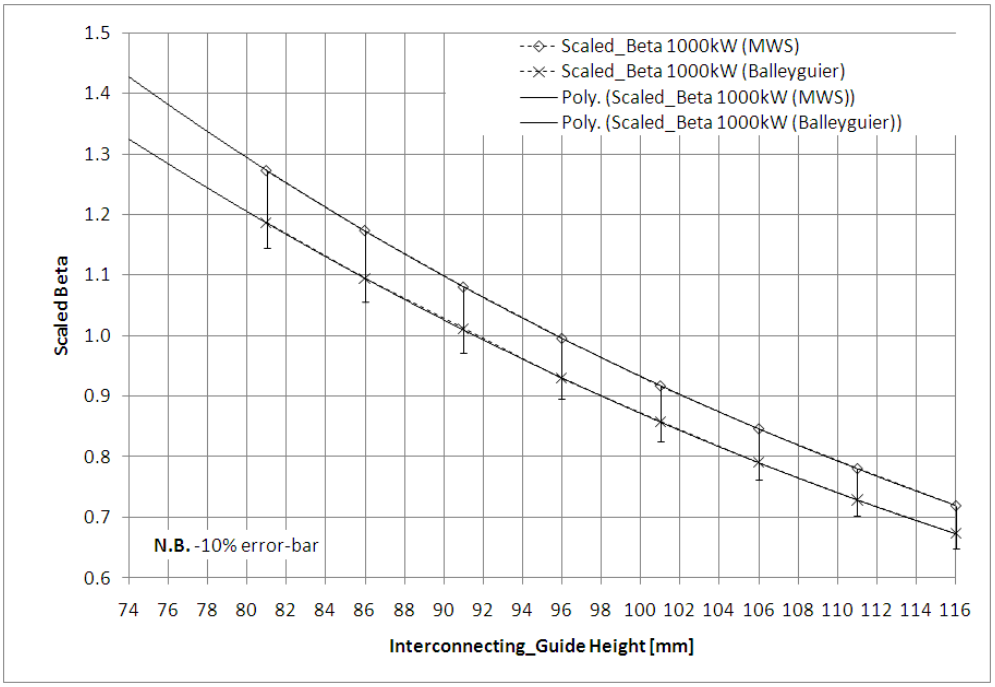

Figure 4 Coupling parameter over IWG height.

In order to reach the optimum value for power transfer at beta equal 1, the height of the IWG is chosen to reach a beta around 1.2, including a 20% margin that can be tuned by increasing or decreasing the length of the short circuit. The waveguide coupler has been simulated with various lengths of the IWG (Figure 4). The optimum height of the IWG for Tank1 is found to be 81 mm.

3. Power dissipation, E_0 field and frequency change

The maximum power loss on the IWG has been calculated to estimate the cooling requirements around the IWG. The calculation has been done on the 22nd and 23rd cell using CST MWS which by default considers 1 J of stored energy, and the result has been scaled with the stored energy from Superfish. Figure 5 shows the geometry of the iris coupler, the IWG and the waveguide. The simulation performed by CST MWS shows a different H field distribution on the 2 different types of structures with and without the half-height WR_2300 waveguide (Figure 6, Figure 7)

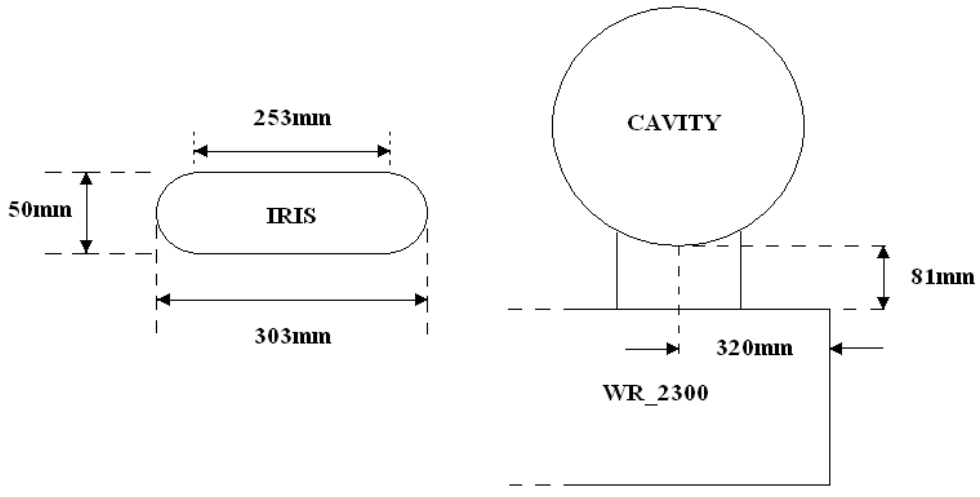

Figure 5 Layout of the cavity connected to the WG through the IWG and iris geometry for Tank1.

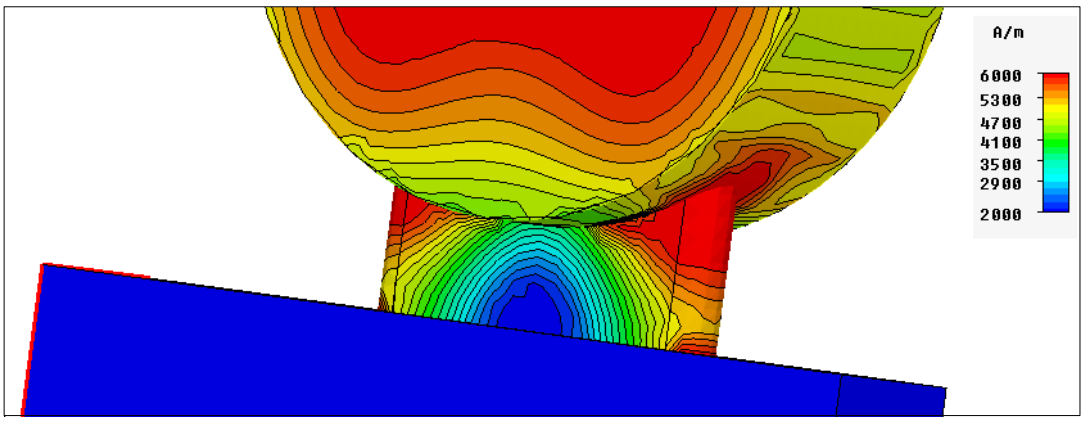

Figure 6 H field (peak) distribution with IWG and WG.

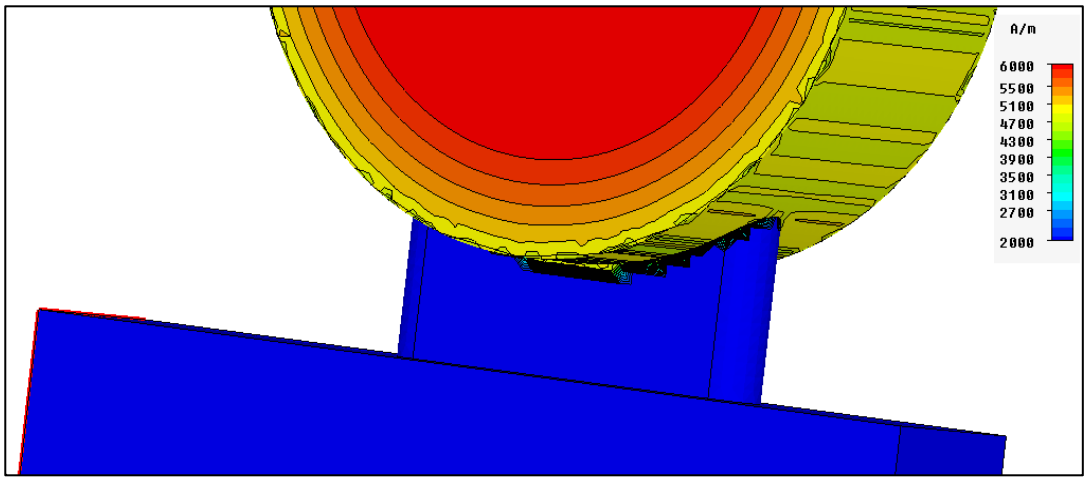

Figure 7 H field (peak) distribution in cells 22 and 23 simulated with the iris being closed at the level of the inner cavity surface.

The power dissipation calculated by CST MWS for the two types of structures and by Superfish for the structure without waveguide is listed in Table 5:

Table 5

	Power without WG (peak) [kW]	Power with WG (peak) [kW]
CST MWS	147.91	154.60
Superfish	157.12[5]	N/A

The CST MWS power dissipation for the structure with and without WG is within 6% of the Superfish simulation. It is important to note that the simulations have been carried out with the same FEM mesh grids and thus the same number of mesh cells. Figure 6 and Figure 7 show that the simulated geometry is the same, but in the case without WG the volume of the WG and of the IWG has been filled with Perfect Electric Conductor (PEC). Furthermore it is important to evaluate the shunt impedance in the two different cases i.e. the ratio V_o^2/P using the average E_z field along the structure. Figure 8 shows the E_z field for the two structures from high energy (HE) to low energy (LE):

[5] Superfish power (peak) is normalized to the 0.55 J stored energy

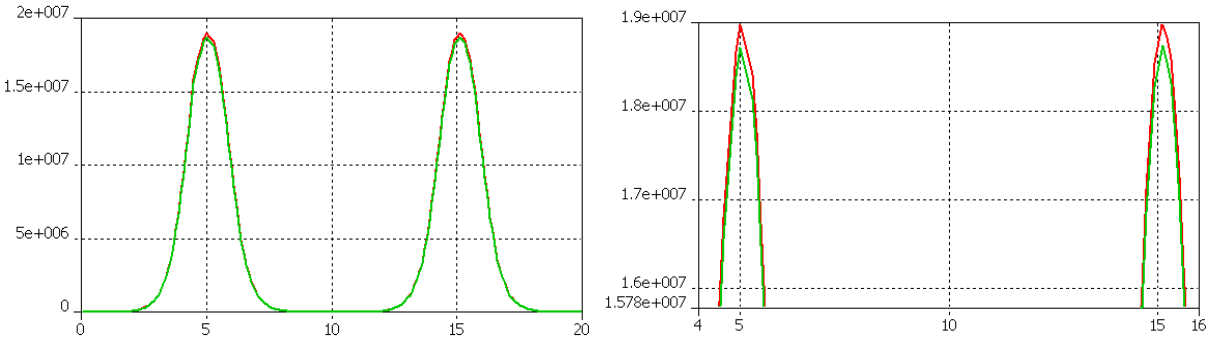

Figure 8 E_z field from cell 23 to cell 22 (i.e. from HE to LE) (left) and magnification (right) with WG (green) and without WG (red).

The difference in the average accelerating field E_0 between the two cells (22 and 23) in the CST MWS simulations with and without WG is within ±1% as is the case in Superfish calculations. A maximum difference of 1.5% is found between the E_0 of the two CST MWS simulations. In order to have the same average accelerating field in the two cells with a waveguide coupler, the power has to be increased by 3% i.e. 1.3 kW. This amount of power corresponds to 0.25% of the power dissipated on the whole tank.

CST MWS simulations show a change in frequency of 0.165 MHz for the 3.90 m Tank1 while HFSS shows 0.155 MHz. These results correspond to 0.644 MHz·m and 0.604 MHz·m respectively when normalized to unit structure length (Table 6). For a comparison, in the PIMS structure we have a similar frequency variation of 0.576 MHz·m.

Table 6 Frequency variation due to the coupling

Cell 22-23	**CST MWS**	**Superfish**	**HFSS**
***f* [MHz] w/o WG**	350.977	353.750	353.600
***f* [MHz] with WG**	347.780	-	350.600
β	29.43 (27.51 Balleyguier)	-	30.27 (VSWR= β overcoupl.)
scaled *β*	1.27 (1.19 Balleyguier)	-	1.31
Δ*f* [MHz]	3.197	-	3.000
Δ*f* · *m* [MHz · m]	0.644	-	0.604

In order to avoid multipacting, edges need to be rounded. For this reason, the same simulation as shown in Figure 6 but with rounded edges between the tank and the IWG is shown in Figure 9. The power density in W/mm^2 has been calculated without (Figure 10, f = 347.780 MHz) and with rounded edges (Figure 11, f = 347.579 MHz). The latter situation has also been analyzed by an HFSS driven mode transient simulation (Figure 12, Figure 13).

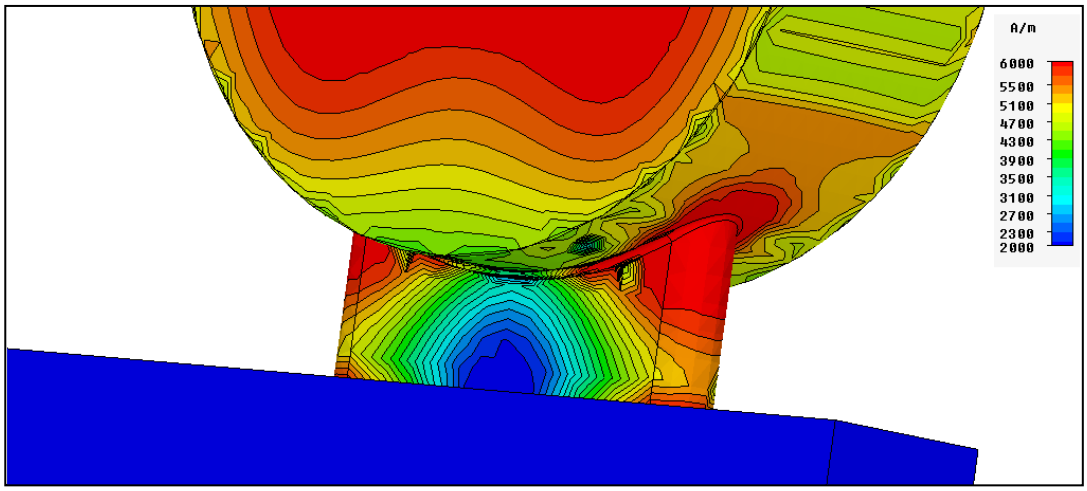

Figure 9 H field (peak) distribution with IWG and WG. The edges between the tank and the IWG are rounded.

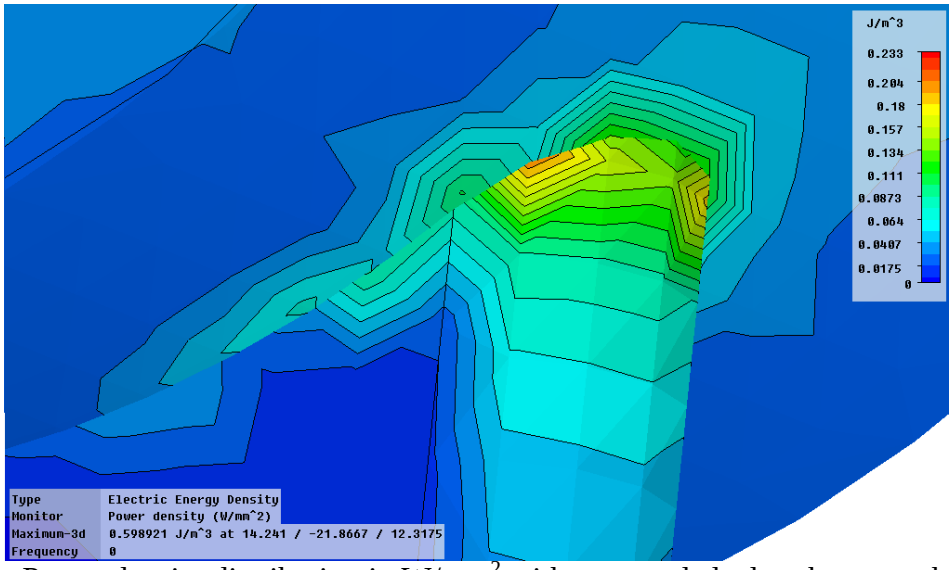

Figure 10 Power density distribution in W/mm^2 without rounded edges between the tank and the IWG (CST MWS).

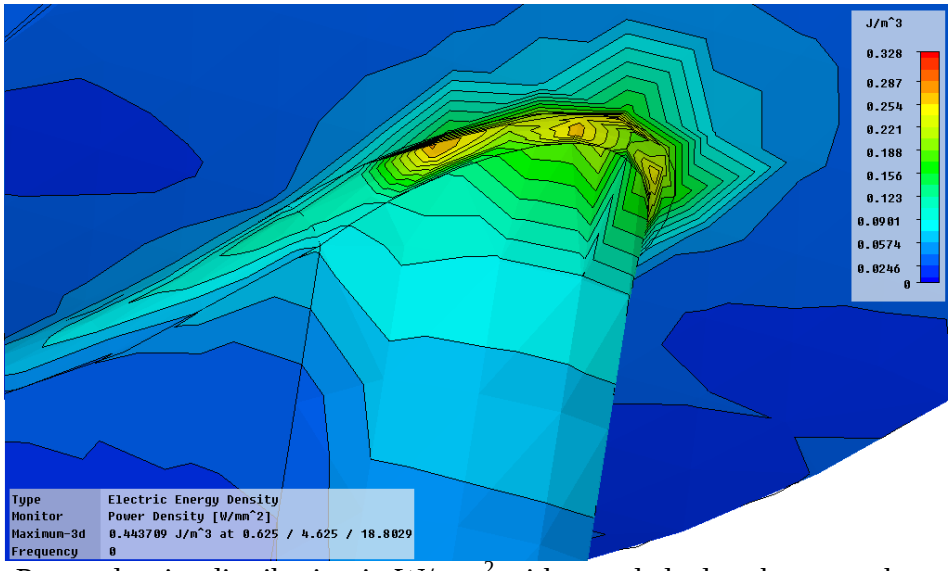

Figure 11 Power density distribution in W/mm^2 with rounded edges between the tank and the IWG (CST MWS).

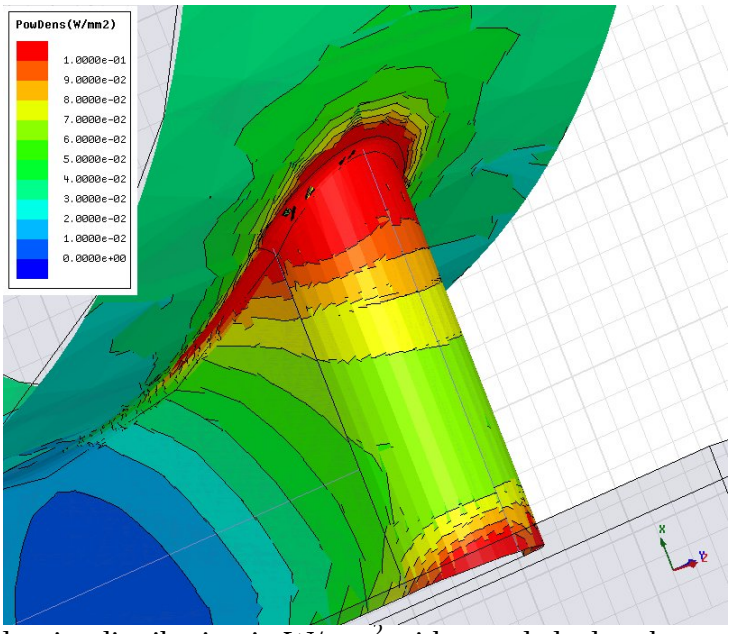

Figure 12 Power density distribution in W/mm^2 with rounded edges between the tank and the IWG (HFSS).

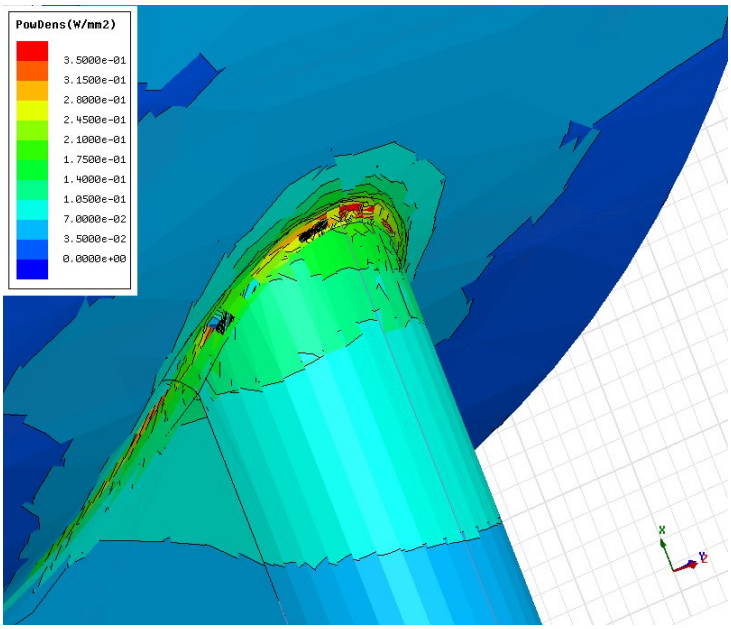

Figure 13 Magnified view of Figure 12.

A maximum power density of about 0.200 W/mm^2 has been found for both codes.

3. Conclusions

The design of the power coupler for the Linac4 DTL structures has been undertaken using 2D and 3D electromagnetic codes. The results scaled from 2-cell simulations are consistent within 10% between simulation methods and with measurements on the prototype reported elsewhere [3]. This is sufficiently accurate for a mechanical design that can be tuned to optimum coupling under beam loading by adjustment of a short circuit. Rounding of edges to avoid multipacting has been taken into account in the simulations.

References

[1] M. Pasini, M. Vretenar, R. Wegner, “CCDTL prototypes: test results”, CARE-Report-2007-036-HIPPI

[2] S. Ramberger et al., “Drift Tube Linac Design and Prototyping for the CERN Linac4”, Proc. LINAC08

[3] G. De Michele, S. Ramberger, J.M. Giguet, J. Marques-Balula, “The Linac4 DTL Prototype: Low and High Power Measurements”, CERN-ATS-Note-2012-003 TECH

[4] P. Balleyguier, “A Straightforward Method for Cavity External Q Computation”, Part. Accelerators, 1997, Vol. 57, 113